

# Numerical Study for Damage Identification in Beams Using Continuous Wavelet Transformation and Convolution Neural Network

Eman R. Bustan<sup>1,\*</sup>, Jaafar K. Ali<sup>2</sup>

<sup>1,2</sup> Department of Mechanical Engineering, College of Engineering, University of Basrah, Basrah, Iraq

E-mail addresses: [emanrah123@gmail.com](mailto:emanrah123@gmail.com), [jaafar.ali@uobasrah.edu.iq](mailto:jaafar.ali@uobasrah.edu.iq)

Received: 3 April 2023; Revised: 4 June 2023; Accepted: 12 June 2023; Published: 30 December 2023

## Abstract

The discovery and identification of damages in engineering structures is very important in the field of engineering maintenance, as it is a great challenge in presenting new methods in measuring vibrations and discovering damages with the development in the field of automation and high accuracy in discovering damages. In this study, natural frequencies and mode shapes of transverse vibration for damage detection in structures are investigated. The study is performed for various crack depth and crack location. And suggested a new technique based on Continuous Wavelet Transform (CWT) and Convolution Neural Network (CNN). The comparison will be done by simulating the oscillations of a cantilever steel beam with and without defect as a numerical case. The proposed new technique proved to outperform classical methods and has achieved a 100% accuracy in the identification of defect position for the data studied.

**Keywords:** Cantilevered beam, Modal analysis, Continuous wavelet transform, Convolution neural network.

© 2023 The Authors. Published by the University of Basrah. Open-access article.

<https://doi.org/10.33971/bjes.23.2.11>

## 1. Introduction

The increasing interest for understanding the vibration behavior to avoid or control the vibration problems at the earliest stage is widely used in most engineering fields, including mechanical ones.

One of the most important of these problems is the identification of damage and cracks in structures. Often times, many researchers and those interested in the field of Modal analysis data ask some questions regarding with modal analysis and how the systems of structures vibrate. So studying the structural dynamic is very essentially to understand and evaluate the performance of any engineering product [1].

So engineers and researchers are often resorting to effective and reliable tool called Modal Analysis Data. The basic concept of Modal Analysis Data is the process of identifying the underlying dynamic properties of a system like natural frequencies, damping factors, and mode shapes [2].

An operational modal analysis (OMA) began in the early 1990's has received great interest in most engineering fields, including aviation, mechanics, and civil, and has applications in various fields, including steel structures, towers, bridges, buildings, etc. Where James, G. H, et. al [3] Natural Excitation Method presented modal identification from output-only measurements in the case of Natural Excitation Technique (NExT). Later in 2002, the two researchers, Wei-Xin Ren and Guido De Roeck [4] proposed the scheme for identification the damage in structures by using modal analysis data and applied this scheme experimentally and theoretically. The results showed the scheme proposed real successive to identify the damage characteristics of structural. And changes in the

dynamic characteristics of a reinforced concrete beam. As well as a potential advantage of the approach is that the modal forces involved in the scheme can be derived directly from any FEM package, and the mode shape expansion is incorporated into the damage assessment procedure using a static recovery technique.

Pankaj Kumar, et. al. (2015) [5] investigated the Modal behavior of Beam-type structures. Included in the investigation are Fixed-Free, Pinned-Pinned, and Fixed-Fixed beams. By using ANSYS simulation for theoretical analysis, and FFT analyzer for experiment. The results demonstrated that natural frequencies derived from simulation and experiment closely match analytical ones.

Amol P. Kale<sup>1</sup> and Dr. S. N. Shelke (2017) [6] proposed a numerical technique for analyzing cantilever beam and improving the strength for different cross section with materials (steel and composite) to get optimum design for beam. The Analytical natural frequency and experimental frequency for the beam were found to have an acceptable and considerable as a good results with max percentage error of 10%. But the natural frequency of Epoxy beam less than mild steel.

N. A. Saleh,., and Z. A Hardan (2018) [7] studied the vibration behavior of cantilevered, simply supported and fixed-fixed beams with a bolted joint of different lap's type and under free and forced vibration. Investigations have been done into the impacts of numerous parameters on natural frequency, mode shape, and amplitude, including beam configuration, pre-torque, angular

speeds, and positions of the motor. The results showed an experimental work present a good agreement with numerical results and with those available in the literature.

Jai Kumar Sharma (2019) [8] presented modal analysis of vibration behavior for different materials types of beam (steel, copper, brass, and aluminum) and pinned-pinned and free-free boundary condition. The modal analysis (natural frequency, mode shapes and damping factors) was done in two part theoretically and experimentally. And from comparison the results, the correlation between the theoretical and experimental was determined to be extremely high.

Yahya. M. Ameen and Jaafar Kh. Ali (2020) [2] studied an experimental modal parameters based on finite element method (FEM) for circular shaft with free ends boundary condition, and then add to shaft two disks as second case. The simulation of Finite Element Method (FEM) was done by software program ANSYS 15 workbench. And the results demonstrated that the experimental method analysis closely matched the numerical results provided by ANSYS, with a maximum percentage of error of 2%.

S H. S, Jasim, and J. K. Ali (2021) [9] introduce new method to measurement the vibration non-contact by using a high-speed camera. The method had been used (the phase-based method) to detect the vibration signal and extract the ODS for the images sequence (video) without the need to use vibration measurements. They conclude that it is reasonable to verify that the ODS and phase difference of an object can be successfully measured with a high-speed camera.

The presence of damage (cracks) in mechanical structures causes a reduction in local stiffness values and an increase in damping factors, hence affecting the vibration response [10].

Z.C. Ong, et. al (2014) [11] introduced an experimental model for detecting fractures on rotor systems by constructing an algorithm to determine the location of cracks based on the first and second natural frequencies. The results suggested that the location of cracks could be determined with confidence and a relatively small error, and the crack severity could be calculated using the damage index

G. Gautier, et. al (2015) [12] identify a new method for updating a finite element method-based subspace fitting methodology for detecting the vibration of structures and localizing damage. And the most important results they reached the finite element method (FE) based subspace approach had been successfully applied to numerically and experimentally beam for the identification damage structures for localizing single and multiple notches at a cheap computational cost.

Shumon Miaa, et. al (2017) [13] proposed the effect of natural frequencies for cracked beam type Fixed- Free, a modal Analysis computationally performed by using Finite Element method (FEM) and software "Abaqus". The results demonstrated that the natural frequency decreased as a result of cracks. The reduction amount relies on the location and size of cracks.

To take a closer look at the continuous wavelet transform (CWT), where it is possible use this transform to get a simultaneous time frequency analysis of a signal.

In the mid-1980s, it began for using the Wavelet analysis to examine seismic signals. Where in 1990s, it began rapidly developing and used for recognition as a useful tool in science

and engineering. Wavelet analysis has been used for many application of engineering and research fields, comprising condition monitoring of machinery, video image compression, seismic signal denoising, characterization of turbulent intermittency, financial index analysis, etc. [14].

Wei Fan and Pizhong Qiao, (2009) [15] studied the damage detection of cantilever plate structures by using algorithm "Dergauss2d" of a two-dimensional of continuous wavelet transform. To demonstrate the efficacy and practicality of this approach, the numerical vibration mode forms of plates with various types of damage are utilized. As demonstrated by the results, it is a viable and successful technique for damage identification of plate- or shell-type structures.

Based on Continuous Wavelet and Wavelet Packet transformations, Mohammad Ali Lotfollahi-Yaghin and Mahdi Koochdaragh (2011) [16] proposed a practical and more useful method for detecting cracks by using (CWT). And they reached to that's the proposed method (CWT) that used research as a powerful mathematical instrument and was more effective for identifying structural stiffness anomalies.

Bülent ORUÇ (2013) [17] examined the effects of magnetic source by using Continuous Wavelet Transform (CWT) based on varied horizontal locations and magnetization vector depths in scale space domain. The results were satisfactory and fairly well determined for semi-infinitely extended experimental bodies.

Roger Serra and Lautaro Lopez (2017) [18] investigated a new approach for identifying structural damage based on difference in deformation of mode shapes of the coefficients of continuous wavelet transform. The results demonstrated that a novel methodology was developed and provided the most accurate results for detecting the location of damage. By comparing the proposed new methodology to well-known and classical methods.

Vahid Shahsavari et al. (2017) [19] proposed and investigated a statistical approach for identifying local beam damage. The beam was evaluated with two boundary conditions (Simply Supported and Fixed ends), the analysis were used continuous wavelet transform to obtain first mode of natural frequency and principal component analysis to recover the major patterns of coefficient change and filter out noise. The results showed that the proposed statistical approaches are highly effective for detecting both occurrence and location of damage and for two boundary condition.

Josué Pacheco-Chérrez et al. (2021) [20] introduced a new method for detecting damage in cantilever beams. Based on two key innovations: first, an image similarity assessment method that makes an efficient use of the full wavelet scalogram and second, an ensemble approach that accounts for material property uncertainty. On the basis of an investigation into experimental data, the results indicated that the newly proposed method has a 100% recognition rate for damage localization.

Recently, an artificial intelligence has witnessed a great development and work to bridge the gap between the capabilities of humans and machines. Researchers and those interested in this field have done amazing things specifically in the field of computer vision.

Developments in computer vision were created with deep learning and mastered over time primarily through one specific algorithm, a convolutional neural network (CNN).

(CNN) is a Deep Learning technique that is frequently utilized in the field of image processing because it is effective at handling with image classification and recognition issues [21]. Yongmei Zhou and Jingwei Jiang (2015) [22] introduced Alexnet Convolutional Neural Network (CNN) to identify in images MNIST digit accelerators by using FPGA. The implementation operates on the MATLAB/CPU Deep Learning Toolbox (CNN) platform. They reached, in the future the implement CNN accelerator implementation will be more desirable in terms of application.

Alex Krizhevsky et al. (2017) [23] trained ImageNet LSVRC-2010 in deep learning Convolutional Neural Network to recognize the 1.2 million high-resolution images consisting of the 1000 distinct classes (CNN). The results indicated that the Convolutional Neural Network (CNN) was able to achieve record-breaking performance on an extremely difficult dataset and by using supervised learning. And network performance degrades if a single convolutional layer is eliminated.

Boukaye Boubacar Traorea, et al. (2018) [24] employed deep learning Convolution Neural Network (CNN) to classify and analysis images for medical image, i.e. microscopy, to confirm or deny the existence of the epidemic pathogen in suspected cases. The suggested CNN architecture provides the best classification results with a classification accuracy of 94%, using 200 Vibrio cholera photos, 200 Plasmodium falciparum images, and 80 images as training and testing data, respectively.

Mingyuan Xin and Yong Wang (2019) [21] proposed an error back propagation approach based on Convolution Neural Network (CNN) to classify images. They evaluated the loss function produced by M3 CE on two depth learning standard databases (MNIST and CIFAR-10). The experimental results demonstrate that M3 CE can increase the cross-entropy and is an efficient supplement to the cross-entropy criterion. M3 CE-CEC has achieved positive outcomes in both databases. And advances the new direction of research into image classification.

The recommended methodology for this study is based on the following points:

Using modal analysis data to study the diagnosis and identification of defects or cracks in structures such as cantilever beams, the cantilevered beam is modeled in the Ansys program, its purpose is to find the theoretical response of the model without or with the presence of a crack or defect. The CWT method is used to analyze the response and performed to determine the response at the interface points in order to increase the number of points until the CWT becomes effective and the results are extracted in the form of images. Created a database from the results to be analyzed. A CNN is built to diagnose defects and their locations based on the database.

## 2. Mathematical model

### 2.1 Beam Modal Analysis

The first stage involves calculating the natural frequencies for the first three modes of the cantilever beam using the software program (Ansys 2022R1). The natural frequencies of beam can be expressed by [25]:

$$\omega_n = \beta_n^2 \sqrt{\frac{EI}{\rho A L^4}} \quad (1)$$

Where ( $\omega_n$ ) is the natural frequency, ( $\beta$ ) is a constant for the type of beam, (E) is the young's modulus, ( $\rho$ ) is the material's density, (I) is the moment of inertia, (A) is the beam's area, and (L) is the beam's length.. Constants ( $\beta$ ) for first three modes of cantilever beam are:

$$\omega_n = (1.8751)^2 \sqrt{\frac{EI}{\rho A L^4}} \quad (2)$$

$$\omega_n = (4.6941)^2 \sqrt{\frac{EI}{\rho A L^4}} \quad (3)$$

$$\omega_n = (7.8548)^2 \sqrt{\frac{EI}{\rho A L^4}} \quad (4)$$

### 2.2 Wavelet Transform

#### 2.2.1 Background of wavelet

The Fourier and Wavelet Transforms are utilized to measure the similarity between the signal and an analyzing function. Comparing their analysis functions, the two transformers are dissimilar. The Fourier transform employs complex exponentials ( $e^{j\omega x}$ ) as its analysis functions. The analysis function in Wavelet Transform is a wavelet( $\psi$ ). The fundamental principles of Wavelet Transform Theory [26, 27] were established for the purpose of constructing Wavelet transforms with certain qualities that make them useful for signal processing.

The mother wavelet ( $\psi$ ) can be written as a zero-mean convolution function:

$$\int_{-\infty}^{+\infty} \psi(x) dx = 0 \quad (5)$$

Analyzing wavelet ( $\psi$ ) (or mother wavelet) is used to construct the CWT function  $\psi_{a,b}(x)$ , which is defined as follows:

$$\psi_{a,b}(x) = \frac{1}{\sqrt{a}} \psi\left(\frac{x-b}{a}\right) \quad (6)$$

Where a, b are parameters represented dilation and translation, respectively.

#### 2.2.2 Continuous Wavelet Transform (CWT) method

Constructing a time-frequency representation of a signal  $x(t)$  using a continuous wavelet transform (CWT) is necessary in order to achieve accurate time and frequency localization. The CWT is described as the following when a shift and compressed or stretched form of a mother wavelet  $\psi(x)$  are compared to the input signal  $f(x)$ , and when the scale parameter  $a>0$  and position b, the CWT is defined as:

$$CWT_f(a, b) = \frac{1}{\sqrt{a}} \int_{-\infty}^{+\infty} f(x) \psi^*\left(\frac{x-b}{a}\right) dx \quad (7)$$

Where  $\psi^*$  is the conjugate of the mother wavelet CWT coefficients  $CWT_f(a, b)$  are obtained by varying the values of the scale parameter a, and the position parameter b, considering the space-scale perspective of signals, it is worthwhile to analyze the wavelet's capacity to respond to small signal shifts or discontinuities. The number of vanishing

moments is a vital characteristic of a wavelet. If  $n$  vanishing moments exist in a wavelet, then:

$$\int_{-\infty}^{+\infty} x^k \psi(x) dx = 0 \text{ for } k = 0 \dots n-1 \quad (8)$$

For any polynomial with orders smaller than the number of vanishing moments, the wavelet returns null values. The number of vanishing moments reflects the wavelet's sensitivity to low-order signals and can be adjusted to consider only specific signal components. It is possible to establish analytically [18] that for a wavelet with  $n$  vanishing moments and a rapid decay, there exists a smoothing function  $u(x)$  defined as follows:

$$\psi(x) = \frac{d^n \theta(x)}{dx^n}, \int_{-\infty}^{+\infty} \theta(t) dt \neq 0 \quad (9)$$

A wavelet with  $n$  vanishing moments, therefore can be expressed as  $n^{\text{th}}$ -order derivative of the smoothing function  $\theta(x)$ . Coefficients of the Continuous Wavelet Transform can be stated as:

$$CWT_f(a, b) = \frac{1}{\sqrt{a}} \int_{-\infty}^{+\infty} f(x) \psi^* \left( \frac{x-b}{a} \right) dx \quad (10)$$

$$= \frac{1}{\sqrt{a}} \int_{-\infty}^{+\infty} f(x) \frac{d^n \theta}{dx^n} \left( \frac{x-b}{a} \right) dx \quad (11)$$

$$= \frac{a^n}{\sqrt{a}} \int_{-\infty}^{+\infty} \frac{d^n}{dx^n} \left( f(x) \theta \left( \frac{x-b}{a} \right) \right) dx$$

The previously mentioned wavelet transform is dependent on the  $n^{\text{th}}$  derivative of the signal function  $f(x)$  that has been smoothed by the function  $u(x)$  at the scale  $a$ . Detecting singularity in a signal function  $f(x)$  is then possible by locating the abscissa where the maxima of the wavelet transform modulus converge at fine scales [26]. In the scenario under consideration, the transition in  $f(x)$  will be induced by a crack, and this is the precise identification approach given.

### 2.2.3 Mode shape refinement and differentiation

This paper proposes a strategy based on the detection of damage revision using CWT. By adding the coefficients of the CWT of the difference between the structure's undamaged and damaged mode **shape**. Then, the difference between the extended refined modal shapes is computed; in this study, the modal shapes are:

$$\phi_{dif}(x) = \phi_{dam}(x) - \phi_{undam}(x) \quad (12)$$

After getting the difference between the two modal shapes undamaged and damaged, this difference is given a Wavelet Transform. The previous step for the  $i^{\text{th}}$  mode shape is written as:

$$CWT(a, b) = \int_{-\infty}^{+\infty} \phi_{dif}^i(x) \frac{1}{\sqrt{a}} \psi^* \left( \frac{x-b}{a} \right) dx \quad (13)$$

### 2.2.4 Addition and weighting of mode shapes

The modal shapes that do not change their natural frequencies are almost not taken into account since they do not bring new information; what is more, they could become a source of noise. So the weighting of the coefficient is used to emphasize the most sensitive mode shapes. It is assumed that when the change in natural frequency is high, the difference between modal shapes will also be important:

$$CWT_{weighted}^i(a, b) = CWT^i(a, b) * \left( 1 - \frac{w_{undam}^i}{w_{dam}^i} \right)^2 \quad (14)$$

where  $w_{undam}^i$  and  $w_{dam}^i$  represent the inherent frequencies of the mode shape in undamaged and damaged states, respectively.

The normalized version of the CWT coefficients will be evaluated to detect and localize structural deterioration. According to the prior analysis, any sudden change in the coefficients will be interpreted as the result of structural deterioration.

### 2.3 Neural Convolutional Network CNN

Convolutional Neural Networks (CNN) are a subtype and special of artificial neural networks created primarily for image processing and recognition by substituting general matrix multiplication with convolution in at least one of its layers [27]. CNNs typically consist of three layers: convolutional, pooling, and fully-connected [28]. As depicted in figure 1.

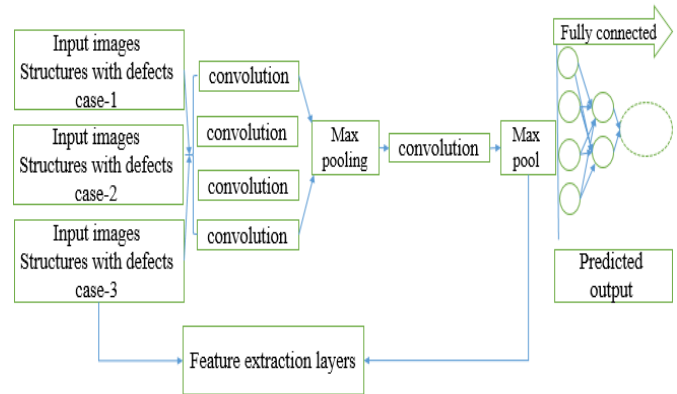


Fig. 1 general operation of CNN.

#### 2.3.1 Convolutional Layer

Convolution layer is the fundamental building component of a CNN, consisting of a set of filters or (kernels) that can be learned and applied to the local image patch. It is effective for abstraction when examples of latent concepts can be separated linearly.

It would be useful to clarify what was intended by the term "convolution," since it is used to convey mathematical principles and ideas regarding the strategy and process of feature modification. In mathematics, specifically algebraic topology, convolution is a mathematical operation that transforms two functions ( $u$  and  $v$ ) into a third function, which is typically considered as a transformed version of one of the starting functions. In the case of two real or complex functions,  $u$  and  $v$ , the convolution is an additional function, typically denoted  $u * v$  and defined as [29]:

$$(u * v)(x) = \int_{-\infty}^{+\infty} u(x-v) v(t) dt \quad (15)$$

The convolution satisfies a number of algebraic properties (such as commutativity, associativity, distributive identity, and multiplicative identity) in order to preserve the qualities of the associated geometric images.

#### 2.3.2 Pooling Layer

Pooling Layer is a non-linear down sampling technique. There are numerous nonlinear functions for implementing pooling, with max pooling being the most used. It divides the input image into a series of rectangles and returns the maximum value for each sub region. By lowering the number of

connections between convolutional layers, it reduces the computational load [30].

### 2.3.3 ReLU Layer

ReLU Layer is an abbreviation for corrected linear unit, and it applies the non-saturating activation function by setting negative activation map values to zero [31].

$$f(x) = \max(0, x) \quad (16)$$

And the most important common function, such as the saturated hyperbolic tangent and the sigmoid function, can be employed to improve nonlinearity. ReLU is frequently favored over other functions since it trains neural networks significantly quicker without sacrificing generalization accuracy. See figure 2.

$$f(x) = \tanh(x) \quad (17)$$

$$f(x) = \frac{1}{(1 + e^{-x})} \quad (18)$$

ReLU results in a neural network that is trained multiple times faster without affecting generalization accuracy significantly.

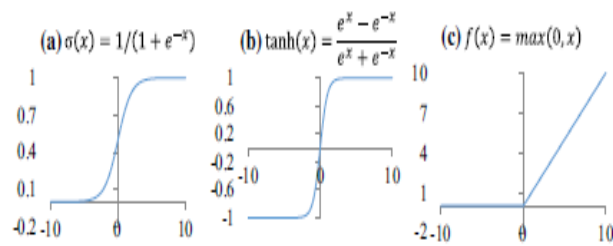


Fig. 2 Activation function. (a) sigmoid, (b) tanh, and (c) ReLU.

### 2.3.4 Fully connected layer

After the last pooling layer in the CNN process are typically completely connected layers. Neurons in a fully connected layer are coupled to all activations in the preceding layer. This layer operates as a conventional neural network and contains around 90 percent of CNN's parameters. This layer accepts as input the output of the previous pooling layer and generates an N-dimensional vector, where N is the number of classes from which the program must select. It permits the neural network to be fed forward into a vector of a predetermined length. For image categorization, we might feed the vector into specific numeric classes [32]. The output is similarly a number vector.

## 3. Results and Discussion

### 3.1 Exposition of the Numerical Model and Simulation

To calculate the free vibration frequency for various mode shapes, a 3D model of a cantilevered beam is presented. The software (Ansys 2022R1) will employ a 3D model that was created to simulate the deflection of a cracked cantilever beam. Steel beam has the following physical characteristics: modulus of elasticity ( $E=210$  GPa), density  $\rho = 7860 \text{ kg/m}^3$ , and Poisson's ratio  $\nu = 0.3$ . The beam's length ( $L=3\text{m}$ ), width ( $W=0.25\text{m}$ ), and depth ( $H=0.20\text{m}$ ) are depicted in (Figure 3). An open edge crack of type V- shaped, perpendicular to the longitudinal axis, with a uniform depth over the span of the cantilever beam was simulated to analyze crack behavior. In

order to examine the behavior of damage indicators, fifteen different damage scenarios are selected and simulated, where the location and size of the damage are modified as shown in Table 1. The data analysis led to the conclusion that all cracked models should feature a V-shaped notched crack of opening 2 mm.

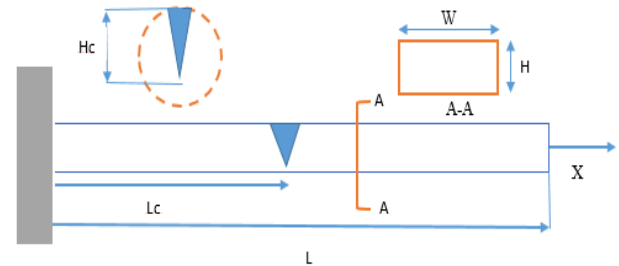


Fig. 3 cantilever beam model.

Table-1: presented cases studies of damage.

Damage case	1	2	3	4	5
Crack location (mm)	500	1000	1500	2000	2500
Crack depth (mm)	50	50	50	50	50
Damage case	6	7	8	9	10
Crack location (mm)	500	1000	1500	2000	2500
Crack depth (mm)	100	100	100	100	100
Damage case	11	12	13	14	15
Crack location (mm)	500	1000	1500	2000	2500
Crack depth (mm)	150	150	150	150	150

The vertical Y displacement of the nodes along the lower edge of the cantilever beam is chosen to indicate the beam's deflection.

Presence of crack causes a complex geometrical property which is difficult to study. Therefore, Ansys 2022R1's 3D tetrahedron element was employed as the FEM type to construct the mesh.

A total of thirty Ansys 2022R1 models are generated for study and discussion of the influence of all damage location and depth (crack). The program controls the number of meshing sites, which varies according on the structure's geometry and the size of the crack. A dense mesh is put close to the crack so that its precise location may be determined (Figure 4).

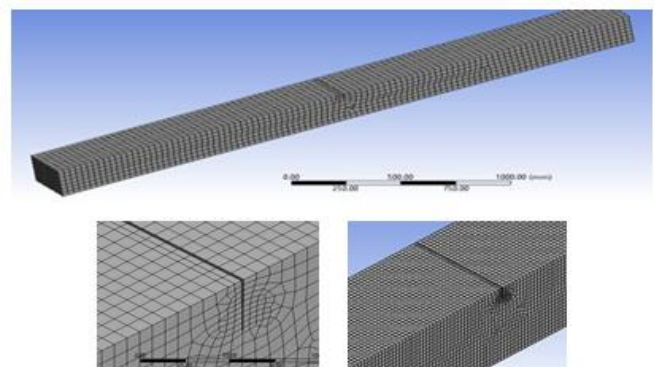


Fig. 4 mesh of Finite-element model.



Table 2 displays the findings of a cracked cantilever beam for different types of meshing influence of mesh size on first natural frequency using the ansys program and three mesh sizes (5mm, 11mm, and 21mm). Observations indicate that combined (Automatic) meshing results in a greater fall in natural frequency, confirming the idea that natural frequency decreases for discontinuous structures. Hence, utilizing both wedge and hexahedral elements simultaneously for local meshing yields the best results in compared to the theoretical outcomes.

**Table 2** A comparison of outcomes for various types and sizes of meshing.

Effect type of mesh size	Mesh size- 5mm	Mesh size- 11mm	Mesh size- 21mm
Automatic	18.557	18.561	18.559
Tetrahedrons	18.395	18.485	18.525
Hex Dominant	18.332	18.389	18.405

### 3.2 Effect of crack location and depth

The influence of the crack is illustrated in Table 3 based on the modes shape and natural frequency at a certain depth of 50 mm and in a variety of places. This table includes information about the crack. The tables make it abundantly evident to that the natural frequency varies from one location to another at the same depth, despite the fact that they are all the same distance apart. For the first mode, the frequency of the crack rises as it advances further away from the end that is fixed. In other words, there is less of a decline in frequency for cracks that are placed closer to the free end, but in the second mode, the frequency begins to decrease and then gradually increases again. It is obvious from looking at the data that the frequency follows a pattern that alternates between growing and shrinking for the third mod. This fact is readily apparent. In addition, the effect of crack depth for a particular crack location has been demonstrated through Table 4 and Figure 5. From these two figures, it is clear that the frequency drops as the crack depth increases, which supports the hypothesis that crack depth has an influence on frequency.

**Table 3** Effect of crack depth on the first three natural frequencies in the event that a crack is present (1500 mm).

Crack depth (mm)	$F_1$ (Hz)	$F_2$ (Hz)	$F_3$ (Hz)
20	18.534	113.33	309.59
50	18.397	109.95	309.55
80	18.089	103.42	309.39
100	17.707	96.802	309.16
150	14.994	72.086	307.66

**Table 4** the influence of crack location on the first three natural frequencies if crack location is (50 mm).

Crack location (mm)	$F_1$ (Hz)	$F_2$ (Hz)	$F_3$ (Hz)
500	17.772	113.61	308.53
1000	18.148	112.54	301.41
1500	18.089	103.42	309.39
2000	18.521	111.11	298.92
2500	18.558	113.54	304.19

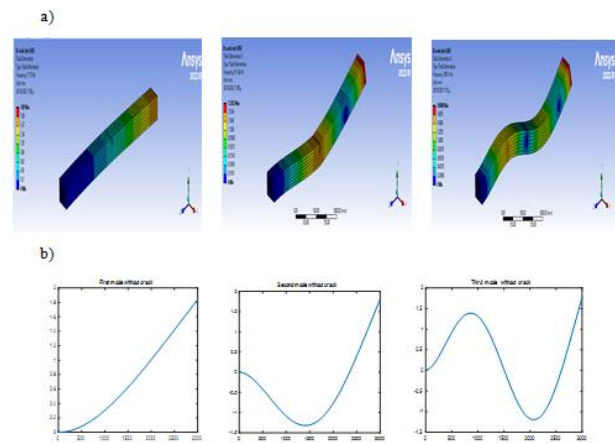
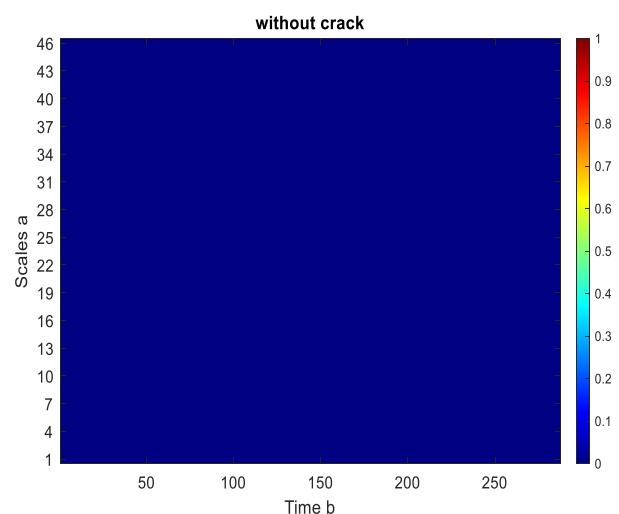


Fig. 5 (a) shows a visual depiction of three modes in the Ansys program on the left, and (b) representation of three modes in the Matlab program on the right.

### 3.2 Analysis of CWT Scalograms for damage identification

The suggested approaches of modes shaped above were also explored by adopting a novel strategy in the treatment of damaged packages, which is the usage of the CWT method according to some damage indicators, which are Modal Assurance Criterion (MAC) based on mode shape data and according to eq (14). The results produced from natural frequencies and modes shapes were analyzed according to the continuous wavelet transform method (CWT), based on the difference in deformation along the beam for both damaged and intact beams.

As for the figures showed the behavior of damage or defect in the beams at different locations and depths, it's obvious from the figures that the CWT method of determining the damage corresponds exactly to the actual situation of the crack in terms of location and depth, and also has the ability to assess the damage correctly and with very high accuracy, regardless of the location and depth of the damage. Where figure 6, 7 and 8 represents the calculated value of the CWT coefficients that were generated using the MATLAB program for different cases of damage at different locations and different depths. In all cases the wavelet function sym1 and scale values ranging from 1 to 46 were used.



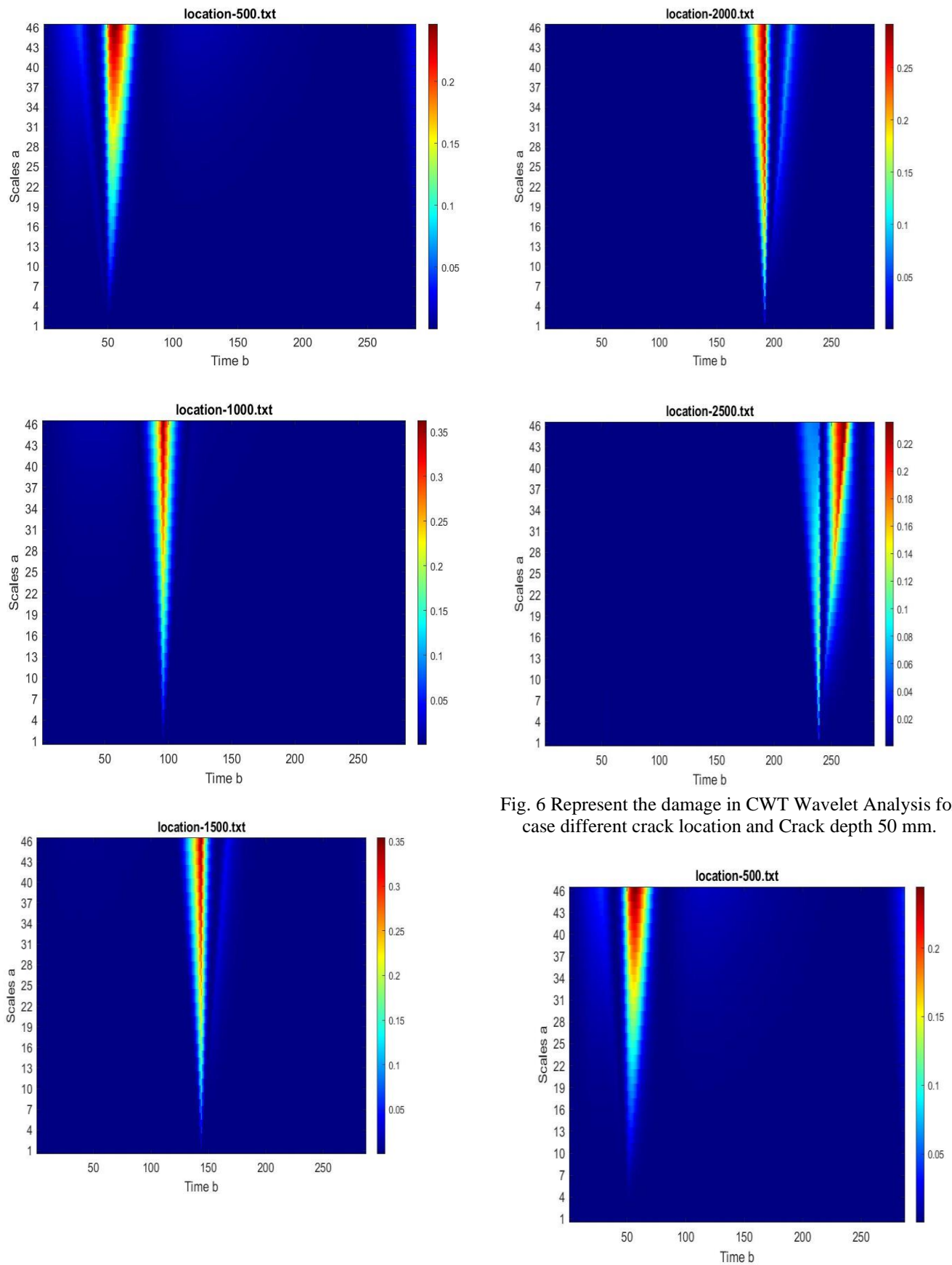


Fig. 6 Represent the damage in CWT Wavelet Analysis for case different crack location and Crack depth 50 mm.

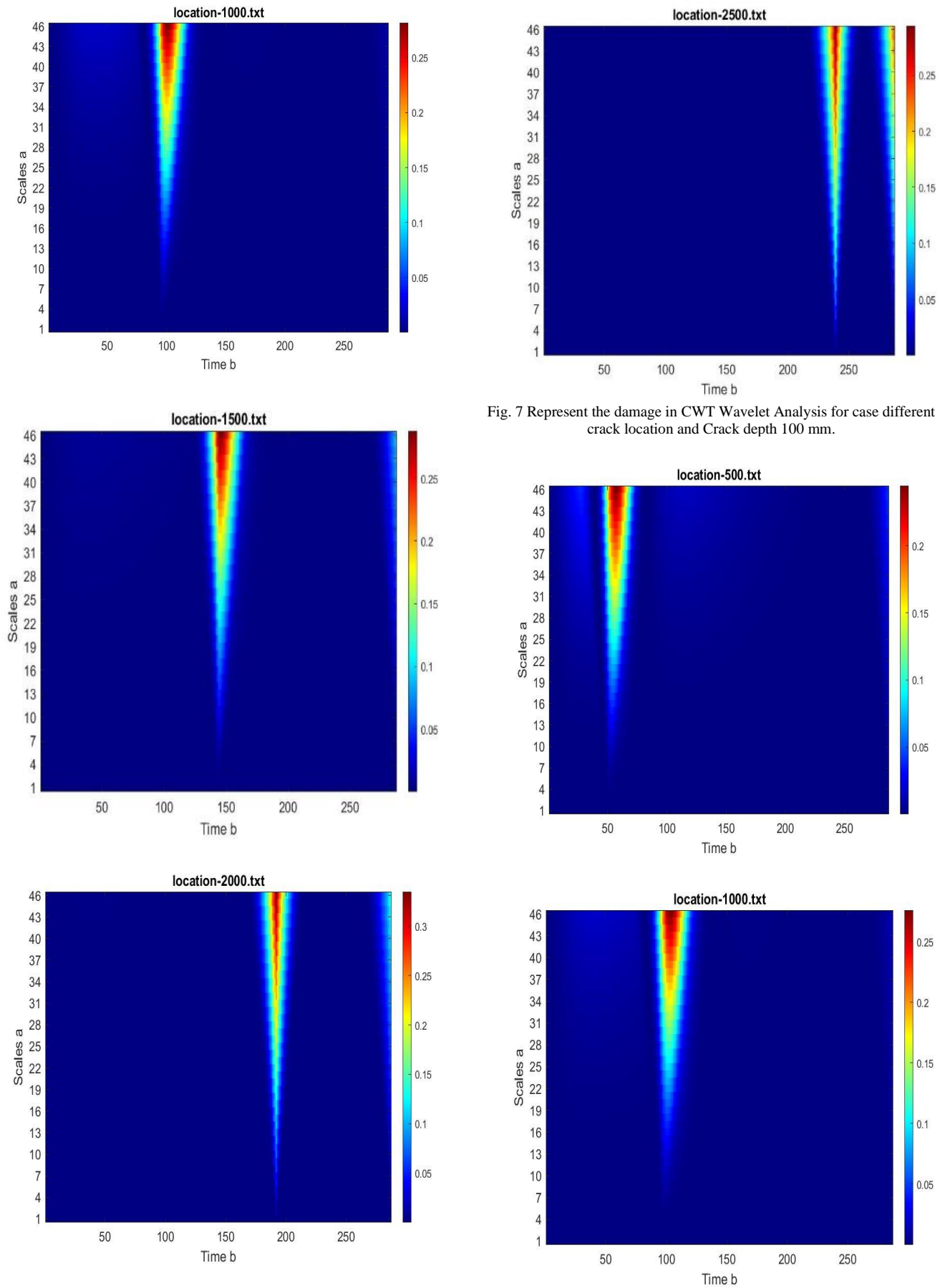


Fig. 7 Represent the damage in CWT Wavelet Analysis for case different crack location and Crack depth 100 mm.



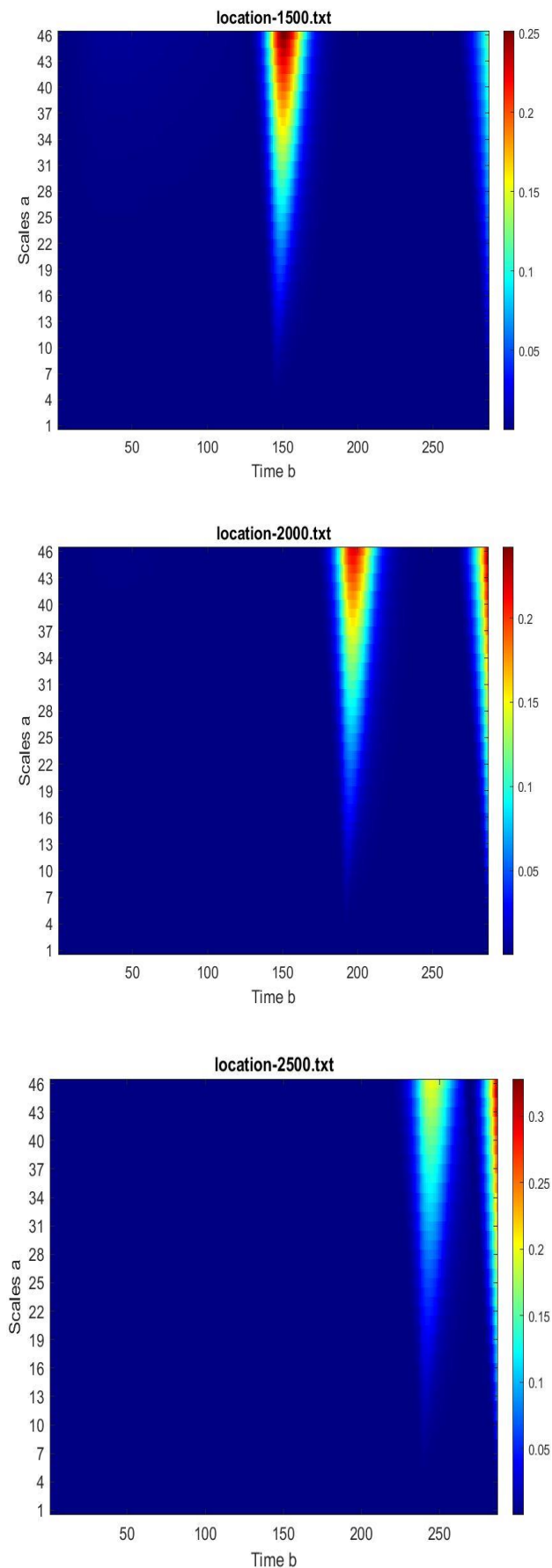


Fig. 8 Represent the damage in CWT Wavelet Analysis for case different crack location and Crack depth 150 mm.

### 3.3 Setup of CNN and creating data base of damaged beams

The network structure in this paper followed Mat-ConvNet (a MATLAB toolbox implementing convolutional artificial neural networks CNNs for computer vision applications), as these networks are widely used in the field of image processing (image net), where images about the location and depth of the crack were fed to the program based on the images generated by Using CWT. In this study, the Alexnet algorithm was employed to differentiate between images.

AlexNet is a convolutional neural network (CNN) architecture developed at the University of Toronto by Alex Krizhevsky, Geoffery Hinton, and others [33, 34]. It was created primarily as a classification tool and won the 2012 ImageNet Large Scale Visual Recognition Challenge (ILSVRC). Alexnet is regarded as one of the pioneering designs in deep learning, and its success in computer vision problems inspired many subsequent structures such as VGG, ResNet, and Inception [35]. This algorithm comprises of 25 layers that are capable of differentiating between 1,000 groups or types. It includes five convolutional layers, three fully-connected layers, and a softmax output layer.

In this study, the same structure of the AlexNet method was utilized, but a straightforward procedure was applied to replace the final three levels of the fully connected layer with a single layer using the transfer layer directive. The CNN's structural parameters are listed in Table 5.

**Table 5:** Structural parameters of Alex net CNN

layer	description
Number of layers	22 layers
Input	Images (jpg) (227*227*3)
Number of convolution layer	5 layers, Conv-1 with stride [4 4] and padding [0 0 0 0], Conv-4-5 with stride [1 1] and padding [1 1 1 1]
Number of max pooling	5, with stride [2 2] and padding [0 0 0 0]
Number of ReLU	5, relu
Number of activation layers	5 layers
Number of dropouts	7, 50 % dropout
Number of fully connected layers	7 layers, weight (4096*4096), Biases (4096*1)
Softmax	softmax
Output	Classification output

In order to prepare a database for the purpose of training the CNN neural network, 30 images were generated for each of the cases of damage that were discussed, and the table shows the number of cases that were discussed, as well as the learning values.

Table 6 shows the nodes where the different damages were located. Separate the data into sets for training and validation. 70% of the photos should be used for training, whereas 30% should be used for validation. Figure 9 illustrates how to construct the database for each of the examined damage instances. As for Figure 10, it shows the results of CNN Neural Network, where the figure shows the accuracy of the

algorithm in recognition, and its results are highly accurate in recognizing each class of damage used, and this is evident through the confusion matrix.

**Table 6:** classification and results of multiple damage of Alex net CNN

properties	description
Number of classes	5 classes (recognize crack location)
Number of image for each class	30 images
Learning rate	$1 \times 10^{-4}$
Number of epoch	6 epoch
Range pixel	[-30 30]

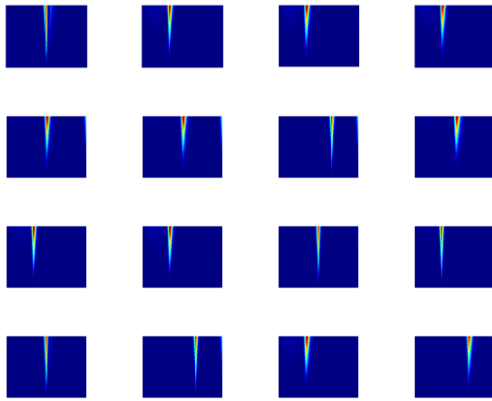
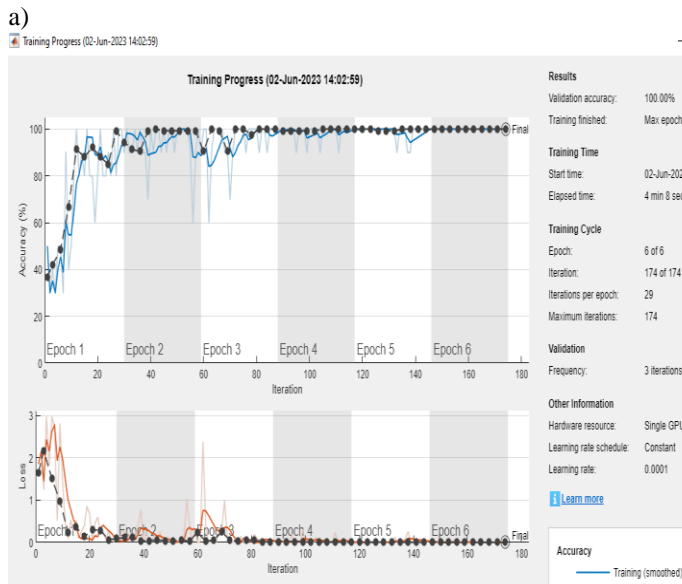


Fig. 9 An images of database for CWT damage beam for different crack location.



b)

Confusion Matrix

Output Class	1000mm	1500mm	2000mm	2500mm	500mm	
1000mm	10 20.0%	0 0.0%	0 0.0%	0 0.0%	0 0.0%	100% 0.0%
1500mm	0 0.0%	10 20.0%	0 0.0%	0 0.0%	0 0.0%	100% 0.0%
2000mm	0 0.0%	0 0.0%	10 20.0%	0 0.0%	0 0.0%	100% 0.0%
2500mm	0 0.0%	0 0.0%	0 0.0%	10 20.0%	0 0.0%	100% 0.0%
500mm	0 0.0%	0 0.0%	0 0.0%	0 0.0%	10 20.0%	100% 0.0%
	100% 0.0%	100% 0.0%	100% 0.0%	100% 0.0%	100% 0.0%	100% 0.0%
	1000mm	1500mm	2000mm	2500mm	500mm	
	Target Class					

c)

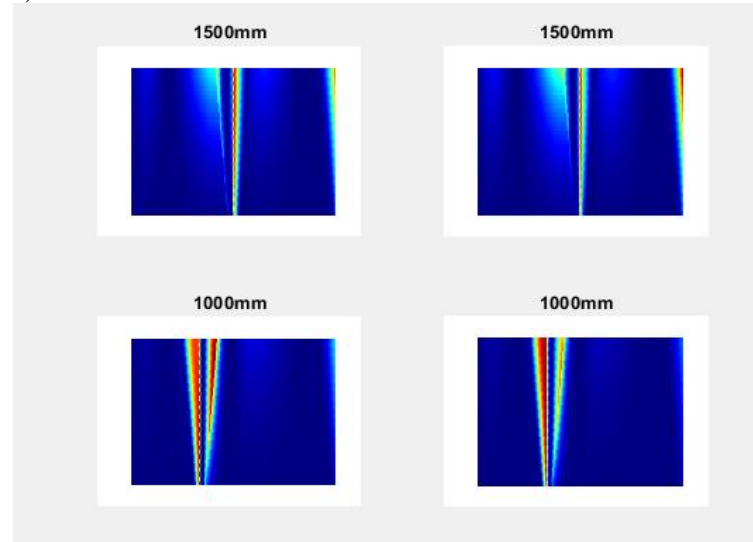


Fig. 10 Results of CNN network classification of damage for different crack location. (a) Accuracy, (b) Confusion matrix and (c) Number of classes of CNN.

## 4. Conclusion

On the basis of modal analysis, a novel method for the reliable detection of the location of a localized damage feature along a cantilever beam has been given. This is based on calculating the differences between the refined modal shapes and those corresponding to the safe state of the structure are afterwards computed. In addition, this method utilizes the most recent technology in Continuous Wavelet Transform (CWT) to detect damage, as it is able to do multiscale analysis on various mode forms. The resultant coefficients are weighted in accordance with the variations in the natural frequencies, enabling full utilization of the information contained in the scalogram of the wavelet-transformed mode shape differences. The CNN image processing method was utilized to swiftly detect and pinpoint damage during the final neural network processing stage. Based on the findings of this study, the following inferences can be made:

The natural frequency decreases due to the presence of cracks. The amount of reduction depends on the location and size of the incisions. For a given crack location, the natural frequencies of the cracked beam are inversely proportional to the depth of the crack.

Continues Wavelet Transform CWT has the most solid performance in calculating the effect of damage indicators and evaluating them correctly. CNN is reliable in identifying the exact location and severity of structural damage. And as for results, the proposed algorithm of AlexNet can predict it with 100% efficiency in all samples studied. The present work focuses on beams with simple geometry and modular damage feature. In the future, experimental data will be used to test the methodology's efficacy in real-world situations.

## Reference

- [1] P. Avitabile, "Experimental modal analysis," *Sound and vibration*, vol. 35, no. 1, pp. 20-31, 2001. DOI: [10.1007/978-3-031-79729-3\\_5](https://doi.org/10.1007/978-3-031-79729-3_5)
- [2] Y. M. Ameen and J. K. Ali, "Theoretical and experimental modal analysis of circular cross-section shaft," in *IOP Conference Series: Materials Science and Engineering*, 2020, vol. 745, no. 1: IOP Publishing, p. 012066. DOI: [10.1088/1757-899X/745/1/012066](https://doi.org/10.1088/1757-899X/745/1/012066)
- [3] G. H. James, T. G. Carne, J. P. Lauffer, and A. R. Nord, "Modal testing using natural excitation," in *Proceedings of the international modal analysis conference*, 1992: Sem Society for Experimental Mechanics Inc, pp. 1208-1208. <https://www.researchgate.net/profile/Thomas-Carne>.
- [4] W.-X. Ren and G. De Roeck, "Structural damage identification using modal data. II: Test verification," *Journal of Structural Engineering*, vol. 128, no. 1, pp. 96-104, 2002. [https://doi.org/10.1061/\(ASCE\)0733-9445\(2002\)128:1\(96\)](https://doi.org/10.1061/(ASCE)0733-9445(2002)128:1(96))
- [5] P. Kumar, T. Vispute, A. Sawant, R. Jagtap, and G. Dalvi, "Modal analysis of beam type structures," *International Journal of Engineering Research and Technology*, vol. 4, no. 4, pp. 650-654, 2015. <https://doi.org/10.1155/2021/8847771>
- [6] S. Shelke, "Static/Modal Analysis of Cantilever Beam," *International Journal of Advance Research and Innovative Ideas in Education*, vol. 3, no. 4, 2017. <https://www.researchgate.net/profile/Damir-Hodzie/publication/357887609>.
- [7] N. A. Saleh and Z. A. Hardan, "Study the Effected Parameters on Vibration Analysis of Cantilever Beam with a Bolted Joint," *Basrah Journal for Engineering Science*, vol. 18, no. 2, 2018. DOI: [10.33971/bjes.18.2.3](https://doi.org/10.33971/bjes.18.2.3)
- [8] J. K. Sharma, "Theoretical and experimental modal analysis of beam," in *Engineering Vibration, Communication and Information Processing: ICoEVCI 2018*, India, 2019: Springer, pp. 177-186. DOI: [10.1007/978-981-13-1642-5\\_16](https://doi.org/10.1007/978-981-13-1642-5_16)
- [9] H. S. Jasim and J. K. Ali, "Detecting Vibration Problems in Machines and Structures Using Motion Capturing by Camera," *Basrah Journal for Engineering Sciences*, p. 38, 2021. <http://dx.doi.org/10.33971/bjes.21.1.6>
- [10] M. Ö. Aydoğan, "Damage detection in structures using vibration measurements," *Middle East Technical University*, 2003. <https://etd.lib.metu.edu.tr/upload/1058809/index.pdf>
- [11] Z. Ong, A. Rahman, and Z. Ismail, "Determination of damage severity on rotor shaft due to crack using damage index derived from experimental modal data," *Experimental Techniques*, vol. 38, pp. 18-30, 2014. DOI: [10.1111/j.1747-1567.2012.00823](https://doi.org/10.1111/j.1747-1567.2012.00823)
- [12] G. Gautier, J.-M. Mencik, and R. Serra, "A finite element-based subspace fitting approach for structure identification and damage localization," *Mechanical Systems and Signal Processing*, vol. 58, pp. 143-159, 2015. DOI: [10.1016/j.ymssp.2014.12.003](https://doi.org/10.1016/j.ymssp.2014.12.003)
- [13] M. S. Mia, M. S. Islam, and U. Ghosh, "Modal analysis of cracked cantilever beam by finite element simulation," *Procedia engineering*, vol. 194, pp. 509-516, 2017. <http://creativecommons.org/licenses/by-nc-nd/4.0/>
- [14] R. Coifman, Y. Meyer, and M. Wickerhauser, "Wavelets and their Applications. Jones and Barlett, Boston, Ch. Wavelet Anal," *Signal Process*, pp. 153-178, 1992. <https://dl.acm.org/doi/abs/10.5555/119607.119612>
- [15] W. Fan and P. Qiao, "A 2-D continuous wavelet transform of mode shape data for damage detection of plate structures," *International Journal of Solids and Structures*, vol. 46, no. 25-26, pp. 4379-4395, 2009. <https://doi.org/10.1016/j.ijsolstr.2009.08.022>
- [16] M. A. Lotfollahi-Yaghin and M. Koohdaragh, "Examining the function of wavelet packet transform (WPT) and continues wavelet transform (CWT) in recognizing the crack specification," *KSCE Journal of Civil Engineering*, vol. 15, pp. 497-506, 2011. DOI: [10.1007/s12205-011-0925-2](https://doi.org/10.1007/s12205-011-0925-2)
- [17] B. ORUÇ, "Determination of horizontal locations and depths of magnetic sources using continuous wavelet transform," *Yerbilimleri*, vol. 34, no. 3, pp. 177-190, 2013. <https://www.researchgate.net/publication/259519054>
- [18] R. Serra and L. Lopez, "Damage detection methodology on beam-like structures based on combined modal Wavelet Transform strategy," *Mechanics & Industry*, vol. 18, no. 8, p. 807, 2017. <https://doi.org/10.1016/j.engstruct.2016.11.056>
- [19] V. Shahsavari, L. Chouinard, and J. Bastien, "Wavelet-based analysis of mode shapes for statistical detection and localization of damage in beams using likelihood ratio test," *Engineering Structures*, vol. 132, pp. 494-507, 2017. <https://doi.org/10.1016/j.engstruct.2016.11.056>
- [20] J. Pacheco-Chérrez, A. Delgado-Gutiérrez, D. Cárdenas, and O. Probst, "Reliable damage localization in cantilever beams using an image similarity assessment method applied to wavelet-enhanced modal analysis," *Mechanical Systems and Signal Processing*, vol. 149, p. 107335, 2021. <https://doi.org/10.1016/j.ymssp.2020.107335>
- [21] M. Xin and Y. Wang, "Research on image classification model based on deep convolution neural network," *EURASIP Journal on Image and Video Processing*, vol. 2019, pp. 1-11, 2019. <https://doi.org/10.1186/s13640-019-0417-8>
- [22] Y. Zhou and J. Jiang, "An FPGA-based accelerator implementation for deep convolutional neural networks," in *2015 4th International Conference on Computer Science and Network Technology (ICCSNT)*, 2015, vol. 1: IEEE, pp. 829-832. DOI: [10.1109/ICCSNT.2015.7490869](https://doi.org/10.1109/ICCSNT.2015.7490869)
- [23] A. Krizhevsky, I. Sutskever, and G. E. Hinton, "Imagenet classification with deep convolutional neural networks," *Communications of the ACM*, vol. 60, no. 6, pp. 84-90, 2017. <https://doi.org/10.1145/3065386>
- [24] B. B. Traore, B. Kamsu-Foguem, and F. Tangara, "Deep convolution neural network for image recognition," *Ecological informatics*, vol. 48, pp. 257-268, 2018. <https://doi.org/10.1016/j.ecoinf.2018.10.002>
- [25] C. M. Harris and A. G. Piersol, *Harris' shock and vibration handbook*. McGraw-Hill New York, 2002. <http://ndl.ethernet.edu.et/bitstream/123456789/25591/1/309>

- [26] M. E. Taylor, "CHAPTER VIII. Geometrical Optics and Fourier Integral Operators," in *Pseudodifferential Operators (PMS-34)*: Princeton University Press, 2017, pp. 146-191. <https://doi.org/10.1515/9781400886104-010>
- [27] I. Goodfellow, Y. Bengio, and A. Courville, *Deep learning*. MIT press, 2016. DOI: <https://doi.org/10.4258/hir.2016.22.4.351>
- [28] Z. Ma et al., "Fine-grained vehicle classification with channel max pooling modified CNNs," *IEEE Transactions on Vehicular Technology*, vol. 68, no. 4, pp. 3224-3233, 2019. DOI: [10.1109/TVT.2019.2899972](https://doi.org/10.1109/TVT.2019.2899972)
- [29] D. Scherer, A. Müller, and S. Behnke, "Evaluation of pooling operations in convolutional architectures for object recognition," in *Artificial Neural Networks–ICANN 2010: 20th International Conference, Thessaloniki, Greece, September 15-18, 2010, Proceedings, Part III 20, 2010*: Springer, pp. 92-101. <http://www.ais.uni-bonn.de>
- [30] G. E. Hinton, N. Srivastava, A. Krizhevsky, I. Sutskever, and R. R. Salakhutdinov, "Improving neural networks by preventing co-adaptation of feature detectors," *arXiv preprint arXiv:1207.0580*, 2012. <https://doi.org/10.48550/arXiv.1207.0580>
- [31] E. J. Heravi, H. H. Aghdam, and D. Puig, "Classification of Foods Using Spatial Pyramid Convolutional Neural Network," in *CCIA*, 2016, pp. 163-168. <https://books.google.com/books>.
- [32] J. Deng, A. Berg, S. Satheesh, H. Su, A. Khosla, and L. Fei-Fei, "Imagenet large scale visual recognition competition," *ilsvrc2012*, 2012. DOI: [10.1109/ACPR.2015.7486599](https://doi.org/10.1109/ACPR.2015.7486599)